Multi-link Piezoelectric Structure for Vibration Energy Harvesting

Rameen M. Aryanpur and Robert D. White

Tufts University Dept. of Mechanical Engineering, 200 College Ave., Medford, MA, USA 02155

ABSTRACT

Work in piezoelectric vibration energy harvesting has typically focused on single member cantilevered structures with transverse tip displacement at a known frequency, taking advantage of the optimal coupling characteristics of piezoceramics in the 3-1 bending mode. Multi-member designs could be advantageous in delivering power to a load in environments with random or wide-band vibrations.

The design presented in this work consists of two hinged piezoceramic (PZT-5A) beams x-poled for series operation. Each beam measures 31.8mm x 12.7mm x 0.38mm and consists of two layers of nickel-plated piezoceramic adhered to a brass center shim. The hinge device consists of two custom-machined aluminum attachments epoxied to the end of a beam and connected using a 1.59mm diameter alloy steel dowel. A stainless steel torsion spring is placed over the pin and attached to the aluminum body to provide a restoring torque when under rotation. The design is modeled using the piezoelectric constitutive equations to solve for voltage and power for a set of electromechanical boundary conditions. Experimental measurements on the design are achieved by bolting one end of the structure to a vibration shaker and fixing the other to a rigid framework of industrial aluminum framing material. For a given frequency of vibration, power output of the structure can be obtained by measuring voltage drop across a resistive load.

Keywords: Piezoelectric Energy Harvesting, Energy Scavenging, Multi-link, Wide bandwidth, PZT

1. INTRODUCTION

The use of piezoelectric structures to harvest energy from ambient vibrations is an enticing solution to increase the lifespan of low-power sensors in remote locations. Previous work in the field has focused primarily on bimorph piezoceramic cantilevers. These structures are well-suited for energy harvesting in environments in which vibration is transverse to the tip of the cantilever bimorph, as they take advantage of the optimal coupling characteristics of piezoceramic materials in the 3-1 bending mode. Many authors have presented rigorous mathematical models for these structures under base excitation with thorough experimental validation [2,8].

While well suited for harvesting energy from transverse vibrations at constant frequency, cantilever beam energy harvesters do not perform well under random vibration. Cantilever structures suffer extensively from the "Gain-Bandwidth Dilemma," whereby the response of the structure is largely attenuated at frequencies other than resonance [7]. Solutions have been proposed to widen the bandwidth of vibration energy harvesters by implementing active control mechanisms [6,9,14]. Active control mechanisms seek to vary the resonant frequency of cantilever energy harvesters through a variety of methods, including moving the location of a proof mass or varying device stiffness through electrostatic comb drives in response to time-varying vibrations [9]. While generally effective, the added complexity and power requirements required for these systems often renders their utility less than optimal for power-stringent energy harvesting applications. Solutions that forgo use of active components in favor of passive ones are thus very attractive for low power and ultra-low power systems.

Passive design for energy harvesters has been explored in various capacities. One approach is a generator array, where cantilevers of varying geometry are arranged in a single package [5, 12, 15]. Each cantilever acts as an energy harvester with a high Q resonance, therefore the sum of the response from each device produces a wide-bandwidth total response. Non-linear structures have been explored with magnets to alter the natural mechanical response of traditional cantilever structures [1,4]. Designing energy harvesters that utilize bimorphs with boundary conditions other than the clamped-free configuration has also proven effective in widening their bandwidth. For example, Hajati et. al developed a MEMS energy harvester utilizing a clamped-clamped beam with a center proof mass [7]. The device takes advantage of the stretching strain in the beam as opposed to the bending strain, producing a bandwidth in excess of 20% about the first resonant frequency. This increase dwarfs the 1%-2% generally achieved in high Q-factor single-cantilever harvesters.

Aside from the aforementioned generator arrays, little work has been done in the field of multi-bimorph energy harvesters. While generator arrays consist of many independent harvesters to provide a wide-bandwidth response to time-variant vibration, multi-bimorph energy harvesters use mechanically coupled bimorphs to produce the same effect. The coupling between each bimorph allows for more complex frequency response spectra within a small volume. Furthermore, whereas in a generator array only several of the cantilevers are excited by a given input frequency, the coupling between bimorphs in a multi-bimorph design allows for interaction between excited and non-excited members, enhancing the overall response of the device.

2. THEORY OF OPERATION

In order to derive a theoretical model for a multi-bimorph piezoelectric energy harvester, simpler cases must first be considered. Through the modeling of these simple geometries, the expressions derived can be extended for use in analyzing more complex devices.

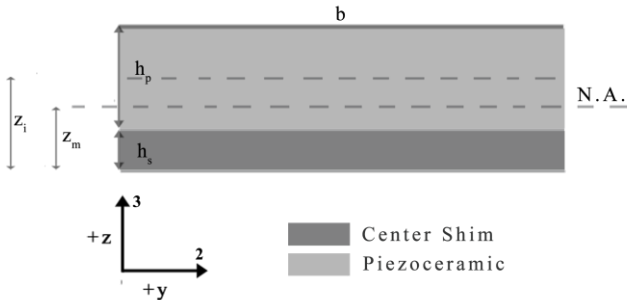### 2.1 Single Layer Cantilever Piezoelectric Energy Harvester With Center Shim

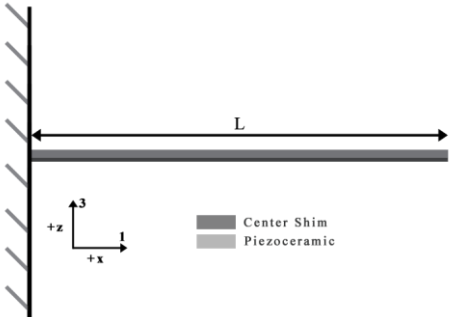Figure 1. Cross-section of single layer cantilever harvester   Figure 2. Side-view of single layer cantilever harvester

A single layer cantilever beam piezoelectric energy harvester in pure bending adhered to a thin shim can be modeled as an alternating current source in series with the intrinsic capacitance of the piezoelectric material. Utilizing the piezoelectric constitutive equations and traditional Euler-Bernoulli beam formulations, expressions for the current source and capacitance can be developed in terms of the material and geometric properties of the piezoelectric material. The determination of these parameters for a single-layer piezoelectric energy harvester facilitates the modeling of more complicated multi-layer piezoelectric energy harvesters.

The piezoelectric constitutive equations express the bidirectional relationship between the mechanical response of a piezoelectric material and an electrical input. The constitutive equations can be expressed in terms of the mechanical stress and strain and the electrical charge and voltage in the piezoelectric material. All formulations are equivalent but involve different constants.

The constitutive equations can be expressed in tensor strain-charge form as,

$$D = E\varepsilon + d\sigma \tag{1.1}$$

Where D is electric displacement $\left(\dfrac{C}{m^2}\right)$, ε is the permittivity of the piezoelectric material $\left(\dfrac{F}{m}\right)$, E is the electric field $\left(\dfrac{V}{m}\right)$, d is the piezoelectric coupling coefficient $\left(\dfrac{C}{N}\right)$, and σ is stress (Pa).

For the plane stress case of a thin piezoelectric harvester in pure bending, the constitutive equation takes the form

$$D_3 = \varepsilon_{33}E_3 + d_{31}\sigma_{11} \tag{1.2}$$

The stress in the piezoelectric layer can be expressed as a function of the Young's Modulus, radius of curvature, and distance from the neutral bending axis, such that

$$\sigma_{11} = Y\frac{(z_i - z_m)}{R_{curv}} \tag{1.3}$$

where Y is the Elastic Modulus of the layer (Pa), R_{curv} is the radius of curvature (m), z_m is the distance to the torque neutral axis (m) from the origin, and z_i is the distance (m) to the center of the ith layer from the origin. For simplicity, the term $(z_i - z_m)$ will henceforth be represented by the more compact term c_d.

The curvature $C_m \left(\dfrac{1}{m}\right)$ is related to the radius of curvature by $R_{curv} = \dfrac{1}{C_m}$ and $C_m = \dfrac{\partial^2 w}{\partial x^2}$, where w is the deflection of the piezoelectric layer perpendicular to the axial direction. The longitudinal stress can therefore be expressed as

$$\sigma_{11} = Yc_d d_{31}\frac{\partial^2 w}{\partial x^2} \tag{1.4}$$

Inserting equation (1.4)into (1.2) yields [13]

$$D_3 = \varepsilon_{33}E_3 + Yc_d d_{31}\frac{\partial^2 w}{\partial x^2} \tag{1.5}$$

To measure the electrical response of a piezoelectric harvester subject to prescribed boundary conditions, a load of known impedance Z is often wired in series with its positive and negative surfaces and the voltage drop across its two leads measured. This setup can be modeled as the simple circuit shown in Figure 3.
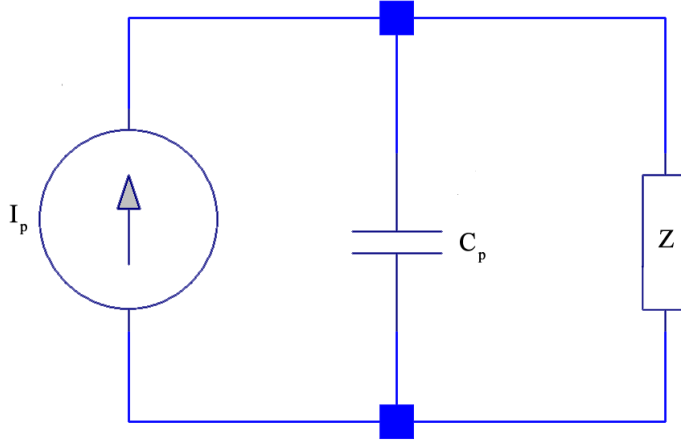
Figure 3. Circuit Model for Single Layer Piezoelectric Harvester

Using Kirkoffs Current Law, the current flow through the circuit can be expressed as

$$I_p = C_p \frac{dV}{dt} + \frac{V}{Z} \tag{1.6}$$

Where I_p is the current generated by the piezoelectric layer, C_p is its capacitance (an intrinsic property of the material), and V is the potential difference across the load. To determine the values of the parameters I_p and C_p, Gauss' Law can be used to obtain

$$\frac{\partial}{\partial t} \int D_3 \cdot dA = \frac{V}{Z}$$

Where the integral is over the area of the surface electrode. Substituting equation (1.5) into the above expression, and considering that the electric field term E_3 can be expressed as $\dfrac{V}{h_p}$, where h_p is the thickness of the piezoelectric layer, yields

$$\frac{\partial}{\partial t} \int \left(\frac{\varepsilon_{33} V}{h_p} + Y c_d d_{31} \frac{\partial^2 w}{\partial x^2} \right) \cdot dA = \frac{V}{Z}$$

Simplifying

$$\frac{\varepsilon_{33} A_c}{h_p} \cdot \frac{dV}{dt} + \frac{\partial}{\partial t} \left(Y c_d d_{31} b \int \frac{\partial^2 w}{\partial x^2} dx \right) = \frac{V}{Z} \tag{1.7}$$

Comparing equations (1.6) and (1.7) allows for determination of the parameters I_p and C_p such that

$$C_p = \frac{\varepsilon_{33} A_c}{h_p}$$

and

$$I_p = \frac{\partial}{\partial t}\left(-Yc_d d_{31} b \cdot \frac{\partial w}{\partial x}\bigg|_{x=0}^{x=L}\right) \tag{1.8}$$

Thus, for a single-layer piezoelectric layer adhered to a thin shim in pure bending, the capacitance of the piezoelectric layer and the current source term have been expressed in terms of the material properties of the harvester and the difference in first derivative of its displacement evaluated at the ends of the electroded section.
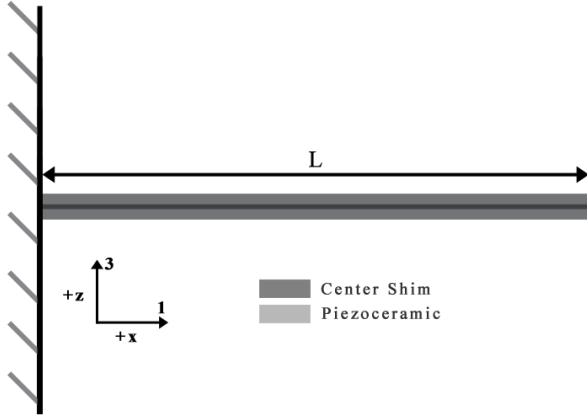
2.2 Bimorph Cantilever Energy Harvester

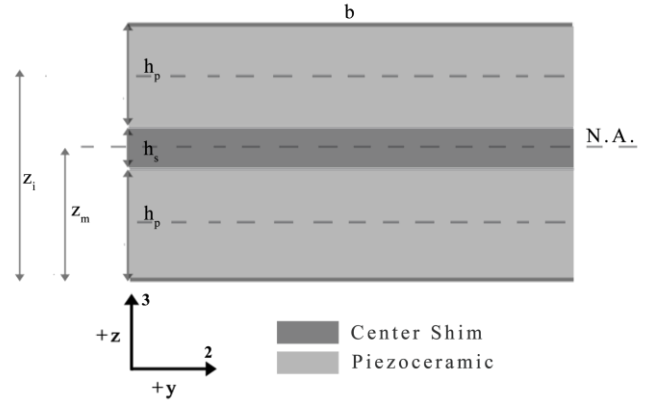Figure 4. Side view of bimorph cantilever harvester   Figure 5. Cross-section of bimorph cantilever harvester

The governing expressions for a bimorph cantilever energy harvester are an extension of those for a single layer cantilever energy harvester. Applying Kirchoffs Current Law to the equivalent circuit for the bimorph (Figure 6) yields

$$I_p = \frac{C_p}{2} \cdot \frac{dV}{dt} + \frac{V}{Z} \tag{2.1}$$

It is important to note that the current source terms in Figure 6 are in the same direction due to the opposite poling of the piezoceramic layers in the series connection case. Utilizing the expressions developed previously for I_p and C_p for the single layer harvester and substituting into equation (2.1) yields

$$\frac{\partial}{\partial t}\left(-Yc_d d_{31} b \cdot \frac{\partial w}{\partial x}\bigg|_{x=0}^{x=L}\right) = \frac{V}{Z} + \frac{\varepsilon_{33} A_c}{2h_p} \cdot \frac{dV}{dt} \tag{2.2}$$

Euler-Bernoulli Beam Theory can be used to develop a second expression to relate displacement w to voltage V, but care must be taken to properly account for the effects of voltage coupling in the piezoelectric layer. Mechanical inputs to the beam generate a voltage potential across the two piezoelectric surfaces so long as they are not under short circuit conditions. This voltage potential imposes a point moment on the boundaries of the beam as outlined by [3]. Thus, for increasing load resistance the mechanical response of the beam is *amplified*, and proper care must be exercised to account for this phenomenon. After some derivation, the governing mechanical equation for the piezoelectric energy harvester is

$$YI\frac{\partial^4 w(x,t)}{\partial x^4} + \rho A_c \frac{\partial^2 w(x,t)}{\partial t^2} = \eta V(t) \cdot \left(\frac{d\delta(x-L)}{dx} - \frac{d\delta(x)}{dx} \right) \qquad (2.3)$$

Where η is a coupling term [2,3] dependent on the wiring of the piezoelectric layers and $\delta(x)$ is the dirac delta function. For series connection, the coupling term is
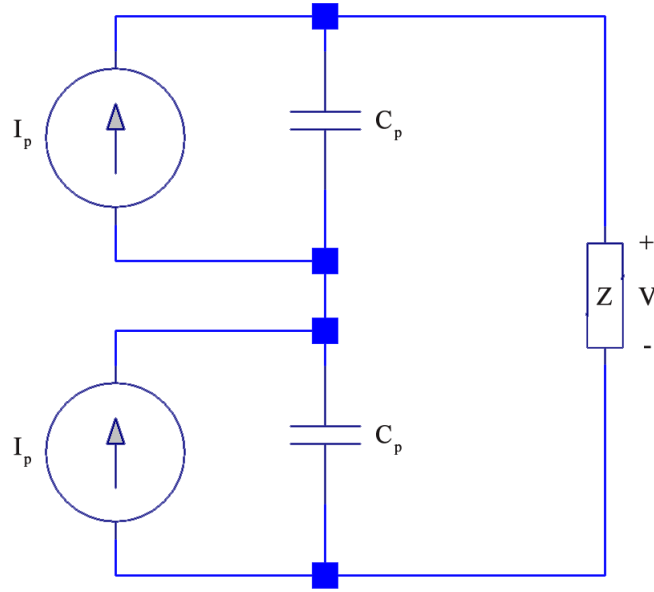
$$\eta = \frac{Y d_{31} h_p b}{2}$$

Figure 6. Circuit model for series-operated Bimorph Piezoelectric Harvester

Thus, the governing electro-mechanical equations for a piezoelectric bimorph are

$$\frac{\partial}{\partial t}\left(-Y c_d d_{31} b \cdot \frac{\partial w(x,t)}{\partial x}\bigg|_{x=0}^{x=L} \right) = \frac{V(t)}{Z} + \frac{\varepsilon A_c}{2h_p} \cdot \frac{dV(t)}{dt} \qquad (2.4)$$

$$YI\frac{\partial^4 w(x,t)}{\partial x^4} + \rho A_c \frac{\partial^2 w(x,t)}{\partial t^2} = \eta V(t) \cdot \left(\frac{d\delta(x-L)}{dx} - \frac{d\delta(x)}{dx} \right) \qquad (2.5)$$

2.3 Two-Bimorph Energy Harvester with Hinge

To widen the frequency response of a piezoelectric energy harvester, a two-bimorph design with a hinge is considered. The hinge consists of two small pieces of machined aluminum, each the width of a single piezo, with a dowel and torsion spring as a connection. The torsion spring is used to couple the mechanical response of each bimorph and add an additional moment to facilitate a wider frequency response.
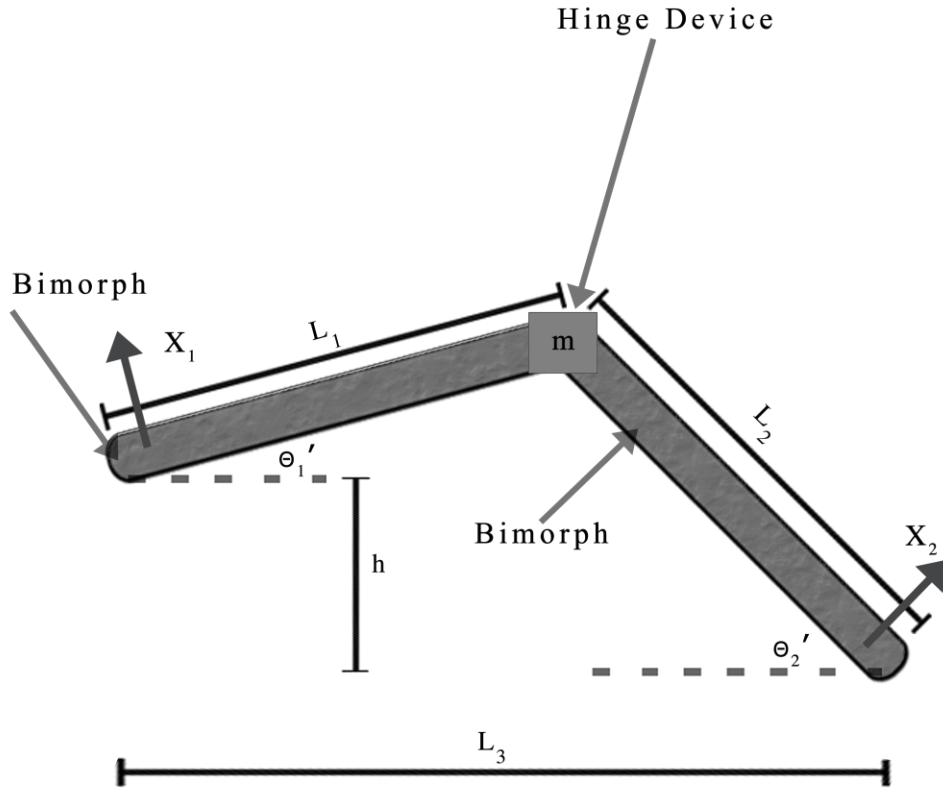
Figure 7. Side-view of two bimorph energy harvester

The two-bimorph harvester can be modeled by an extension of the expressions developed in Section 2.2. Each bimorph is modeled as a single piezoelectric bimorph where the spring coupling is defined by the boundary conditions. The governing equations are then collected in matrix form and solved for the unknowns to generate a particular solution at a specific frequency.

Because the system is assumed to be time harmonic, the governing expressions can be simplified. That is, all time-dependent terms are assumed to be oscillating with known magnitude at known frequency ω. Further, the effect of voltage back-coupling in the piezoelectric layers is absorbed into the boundary conditions as a point moment at the beam's ends, transforming equation (2.5) into a homogeneous ODE. The steady-state governing equations for each bimorph are,

$$-j\omega Y c_d d_{31} b \cdot \left.\frac{W_1(x_1)}{\partial x_1}\right|_{x_1=0}^{x_1=L} = \frac{V_1}{Z} + \frac{j\omega\varepsilon_{33}A_c}{2h_p}V_1$$

$$-j\omega Y c_d d_{31} b \cdot \left.\frac{W_2(x_2)}{\partial x_2}\right|_{x_2=0}^{x_2=L_2} = \frac{V_2}{Z} + \frac{j\omega\varepsilon_{33}A_c}{2h_p}V_2 \qquad (3.1)$$

$$YI_1 \frac{\partial^4 W_1(x_1)}{\partial x_1^{\,4}} - \omega^2 \rho A_c W_1(x_1) = 0$$

$$YI_2 \frac{\partial^4 W_2(x_2)}{\partial x_2^{\,4}} - \omega^2 \rho A_c W_2(x_2) = 0 \tag{3.2}$$

The Euler Bernoulli beam expression is now a 4th order linear, ordinary differential equation, for which the homogeneous solution is known

$$W_1(x_1) = c_1 \cos(\beta_1 x_1) + c_2 \sin(\beta_1 x_1) + c_3 \cosh(\beta_1 x_1) + c_4 \sinh(\beta_1 x_1)$$

$$W_2(x_2) = c_5 \cos(\beta_2 x_2) + c_6 \sin(\beta_2 x_2) + c_7 \cosh(\beta_2 x_2) + c_8 \sinh(\beta_2 x_2) \tag{3.3}$$

where

$$\beta_1 = \left(\frac{\rho A_c \omega^2}{YI_1} \right)^{1/4} \tag{3.4}$$

$$\beta_2 = \left(\frac{\rho A_c \omega^2}{YI_2} \right)^{1/4} \tag{3.5}$$

For each bimorph, a set of three boundary conditions can be defined, two at the clamped end for displacement and slope and one at the hinged end for moment. For the first bimorph these are,

$$W_1\big|_{x_1=0} = X_1 \qquad\qquad W_1{'}\big|_{x_1=0} = 0$$

$$YI_1 W_1{''}\big|_{x_1=0} = \eta V_1 - \kappa(\Theta_1 + \Theta_2 - \Theta_0) \tag{3.6}$$

and for the second ,

$$W_2\big|_{x_2=0} = X_2 \qquad\qquad W_2{'}\big|_{x_2=0} = 0$$

$$YI_2 W_2{''}\big|_{x_2=L_2} = \eta V_2 - \kappa(\Theta_1 + \Theta_2 - \Theta_0) \tag{3.7}$$

Where X_1 and X_2 are the forced normal deflections of the beams at either end, κ is the constant force torsional spring torque, and YI_1 and YI_2 are the effective stiffenss of the beams. The term Θ_0 can be expressed as

$$\Theta_0 = \theta' - \pi + \theta_1{'} + \theta_2{'}$$

Where θ' is the natural rest angle of the spring and θ_1', θ_2' are the inner rest angles as defined in Figure 7. A set of two compatibility conditions can be defined for the displacement of the hinge, as translation of each beam must be equal at that point,

$$L_1 \cos(\theta_1\,') - W_1\big|_{x_1=L_1} \sin(\theta_1\,') = L_3 - L_2 \cos(\theta_2\,') + W_2\big|_{x_2=L_2} \sin(\theta_2\,')$$

$$L_1 \sin(\theta_1\,') + W_1\big|_{x_1=L_1} \cos(\theta_1\,') = -h + L_2 \sin(\theta_2\,') + W_2\big|_{x_2=L_2} \cos(\theta_2\,') \tag{3.8}$$

where the various lengths are taken from Figure 7, and the angles are the undeflected angles, also taken from Figure 7. Finally, taking force balances on the hinge element, including two new variables to represent the axial forces carried by the beams, F_1 and F_2,.

$$F_1 \cos(\theta_1\,') - v_1 \sin(\theta_1\,') - F_2 \cos(\theta_2\,') + v_2 \sin(\theta_2\,') = m\omega^2 W_1\big|_{x_1=L_1} \sin(\theta_1\,')$$

$$F_1 \sin(\theta_1\,') + v_1 \cos(\theta_1\,') + F_2 \sin(\theta_2\,') + v_2 \cos(\theta_2\,') = -m\omega^2 W_1\big|_{x_1=L_1} \cos(\theta_1\,') \tag{3.9}$$

where m is the mass of the hinge fixture, and v_1 and v_2 are the shear at the end of the beams, which are related to the third derivative of the deflection,

$$v_1 = YI \frac{\partial^3 W_1}{dx_1^3}\bigg|_{x_1=L_1}$$

$$v_2 = YI \frac{\partial^3 W_2}{dx_2^3}\bigg|_{x_2=L_2} \tag{3.10}$$

Finally, the complete electromechanical system can be solved for the 12 unknowns,

$$\begin{bmatrix} c_1 & c_2 & c_3 & c_4 & c_5 & c_6 & c_7 & c_8 & V_1 & V_2 & F_1 & F_2 \end{bmatrix}$$

where the algebraic equations are (3.1), (3.6), (3.7), (3.8), and (3.9). This results in a 12 by 12 linear algebraic system to be solved at each frequency ω.

3. EXPERIMENTAL SETUP AND RESULTS

3.1 Single Bimorph Experimental Setup

To assess the validity of the theoretical analysis presented in Section 2, a bimorph piezoelectric beam with a brass center shim was purchased from Piezo Systems, Inc. and tested. The piezoelectric bimorph consisted of two layers of PZT-5A adhered to a brass center shim, as seen in Figure 5. The PZT-5A was fully Nickel-electroded to allow for charge collection across the entire surface. The two layers are wired for series connection and oppositely poled, as modeled in Figure 6.

Table 1. Dimensions of bimorph and relevant piezoelectric parameters [11]

Length	31.8 mm
Width	6.4 mm
Thickness Piezo	.14 mm
Thickness Shim	.10 mm
Youngs Modulus Piezo	50 GPa
Youngs Modulus Shim	40 GPa
Piezoelectric Coupling Coefficient (d_{31})	$-190 \dfrac{pC}{N}$
Relative Permittivity of Piezo	1800

To test the frequency response of the bimorph, a clamping device was designed and fabricated using Type 6061 Aluminum Alloy. The clamping device consisted of two pieces of equal dimensions. A small groove with the same width as the piezoelectric bimorph was milled out of the bottom piece, and the bimorph was placed in the groove and epoxied in place. The top and bottom pieces were screwed together, securing the piezoelectric bimorph. To prevent against electrical shorting between the bimorph and the aluminum, the clamping device was coated with 1.5 microns of Parylene-C, an insulating polymer, using vapor phase deposition techniques.

The clamping mechanism was attached to an impedance head for a B& K Type 1809 Vibration Exciter. The clamping mechanism was capable of rotating with respect to the impedance head so that the angle between the clamp and the vibration exciter could be changed between tests, but could be tightened by two screws and fixed during tests. For testing of the single cantilever bimorph, the clamping device was fixed perpendicular to the vibration exciter.

3.2 Results and Discussion

A frequency sweep was taken on the bimorph using data acquisition hardware and National Instruments LabVIEW 2009. A B&K Type 8001 accelerometer was placed between the shaker and the adaptive head to measure the acceleration at the base of the cantilever bimorph. Two wire leads were soldered to either side of the Nickel-plated PZT surfaces and the voltage across the bimorph was measured.

The frequency response of the bimorph from both the experimental and analytical cases was taken over a range of frequencies. The ratio of voltage response from the piezo in Volts to acceleration of the clamped base in m/s^2 was plotted in decibels as $20 \cdot \log_{10} \left(\dfrac{Piezo\ Voltage\ in\ V}{Base\ Accleration\ in\ m\ /\ s^2} \right)$. The device was swept through a frequency band of 10 Hz – 680 Hz to produce the wide-band response presented in Figure 9.

The first resonance of the piezoelectric bimorph was observed at ~233 Hz, with an amplitude of approximately -1.3 dB. This is equivalent to a voltage sensitivity of 8.46 V/g. Power output is not reported, as power is being dissipated across the 100 $G\Omega$ input impedance of the data acquisition hardware, not across an optimal impedance. Values presented in the literature are generally for power delivered to optimal impedances at resonance. Determination of the optimal impedance at first mode resonance for the device is ongoing.

Several discrepancies are observed between the model and experiment, the most salient of which is a persistent 5 dB gap between the two data sets. Identification of the cause for this discrepancy is ongoing, however, small inconsistencies between reported values of the piezoelectric properties from the manufacturer and actual values, as well as potential alteration of the equivalent spring constant of the piezo from the epoxy in the clamp are suspected to have an effect. For

example, the voltage generated across the piezo layers scales linearly with the piezoelectric coupling coefficient d_{31}, so a 10% error in the reported value of the coupling coefficient would represent a ~1dB drop in the overall response of the bimorph. Quantifying the effect of the epoxy on the spring stiffness is ongoing.

The model predicted a resonant frequency of approximately 215 Hz, while the observed resonant frequency was approximately 230 Hz, a variation of 6.9%. This 6.9% fits within the tolerances expected from small variations in the material properties of the PZT.

The presence of two smaller peaks straddling the largest peak is an additional discrepancy between the model and experiment. The smaller amplitude peaks are thought to be modes of the test structure. Although it was designed to be rigid, the test structure has nut and bolt connections at two locations: between the accelerometer and the exciter attachment and the exciter attachment and the clamp. The connection between the accelerometer and exciter attachment is very rigid, and the loading imposed by the shaker is axial in nature, therefore this connection most likely produces modes at frequencies larger than those observed in Figure 9. Rather, the connection between the exciter attachment and the clamp is most likely producing the extraneous peaks in the frequency sweep. Although the nut and bolt connection between the two pieces was tightened as much as possible, the shaker produces a torque that works to loosen it (Figure 8). The smaller peaks observed in Figure 9 are thought to be a result of the torsional modes of that connection.
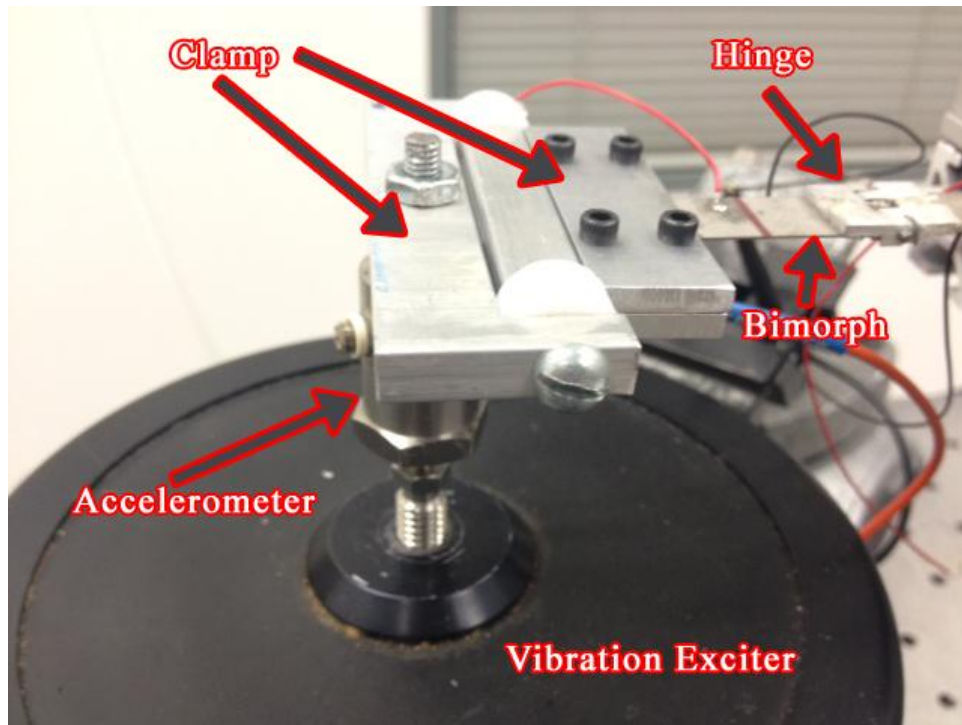

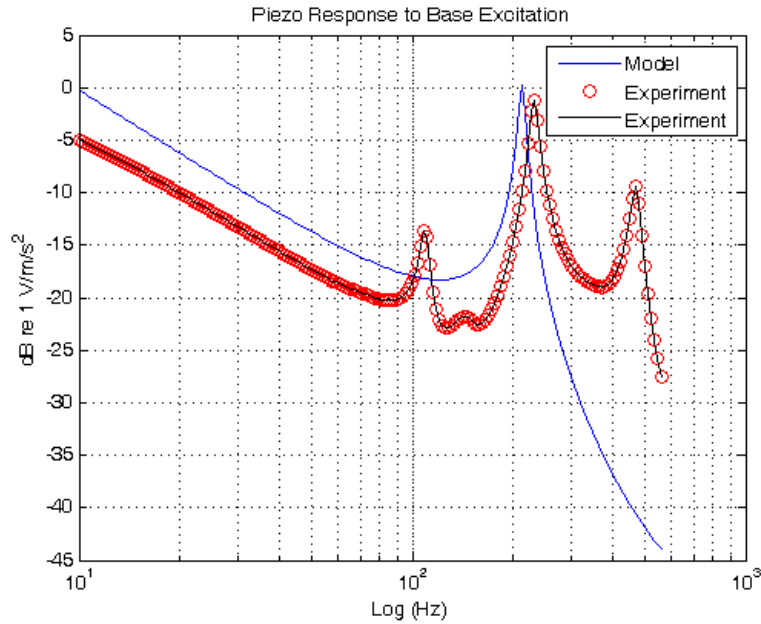Figure 8. Connection between accelerometer, adaptive head, and clamping mechanism.

Figure 9. Theoretical vs. Experimental response of series-connected piezoelectric bimorph from 10 Hz – 680 Hz

3.2 Two Bimorph Experimental Setup

The two bimorph energy harvester is composed of two of the bimorphs used in section 3.1 connected by a hinge. Each bimorph is clamped at one of its ends, with the other attached to the hinge, two small pieces of machined aluminum--each the width of a single piezo--with a 1.59mm diameter aluminum dowel and torsion spring connecting them. The aluminum pieces were required in order to provide a large epoxy contact surface for the bimorphs and to restrict out-of-plane motion. The aluminum portions of the apparatus—those that came in contact with the PZT—were coated with 1.5 microns of Parylene-C to prevent electrical shorting.
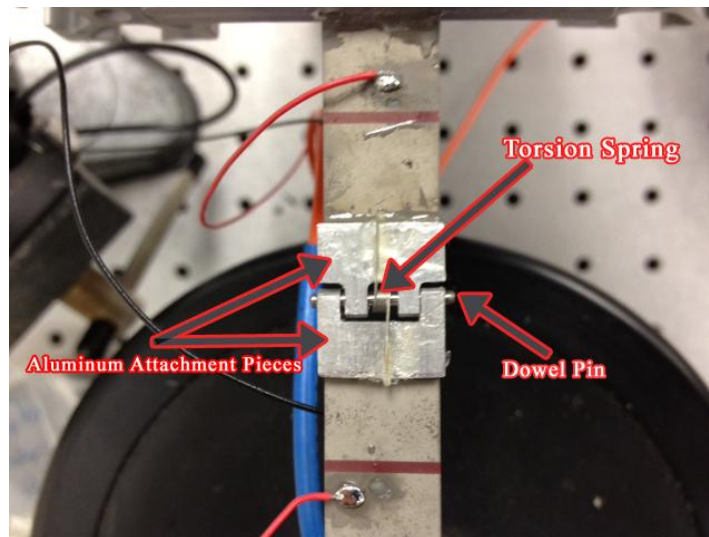

Figure 10. Top view of hinge device with Parylene-coated aluminum attachments, torsion spring, and dowel

The experimental setup for the two bimorph energy harvester uses the same exciter attachment and clamp as the single bimorph, but with an additional structure to support the second bimorph. The structure is constructed of a rigid aluminum framework, to which a clamp identical to the one previously described can be bolted. The clamp is not allowed to rotate, unlike the one connected to the exciter attachment. This provides rigidity to the test structure in an effort to prevent additional extraneous structural modes in the frequency sweep.
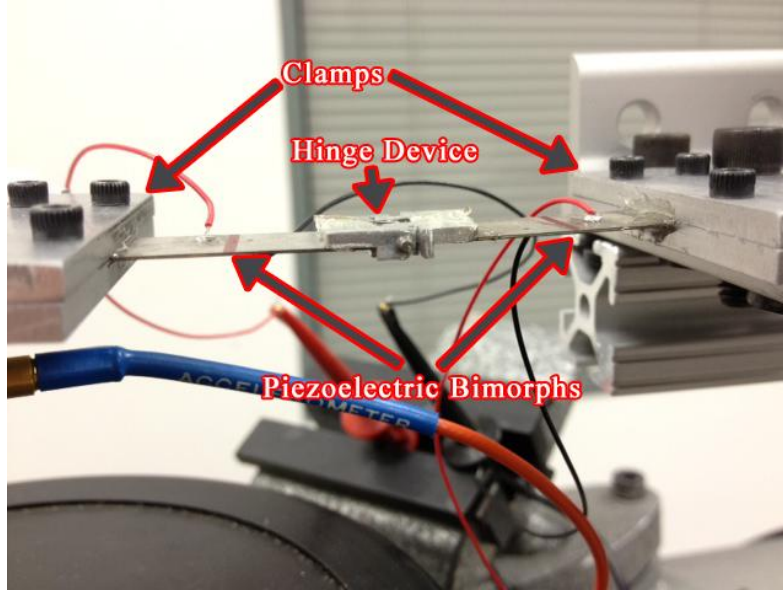

Figure 11. Side view of multi-bimorph device with exciter clamp (left) and rigid clamp (right) visible

As was the case for the single bimorph, wires were soldered to the top and bottom Nickel-plated surfaces to measure the voltage across the piezoelectric device in response to a range of time harmonic base excitations. Because the entire surface was Nickel-plated, charge cancellation due to improper wire placement was not of concern [2], and the exact location of the wires on the surface was irrelevant.

3.2 Two Bimorph Results and Discussion

The two bimorph energy harvester was tested in a flat-flat configuration with the same data acquisition hardware and processing software discussed in Section 3.1.2. The flat-flat configuration is characterized by the inner angles θ_1' and θ_2' in Figure 7 set to zero. In this configuration, the energy harvester is subject to a base excitation from the shaker at one end and fixed at the other, and the torsion spring rotates in accordance with the curvature of the bimorph at their attachment point. The voltage across each bimorph is measured as well as the base acceleration of the bimorph attached to the shaker and the ratio of piezo voltage in volts to acceleration of the clamped base in m/s^2 is plotted in decibels as

$$20 \cdot \log_{10} \left(\frac{Piezo\ Voltage\ in\ V}{Base\ Accleration\ Exciter\ Bimorph\ in\ m\ /\ s^2} \right).$$

The wideband frequency response of the two bimorph device is similar in shape to the single bimorph device, but with several key differences. First, at low frequencies, the two bimorph device has a larger amplitude response that decreases at a steep ~10 dB/decade. At approximately 100 Hz, a small peak occurs similar to the one seen in the single bimorph, but with half the amplitude. The response flattens slightly but still decreases at ~2 dB/decade before hitting another small 5 dB peak at approximately 180 Hz. This peak was not observed in the case of the single bimorph. At 250 Hz, a

strong peak is observed in both bimorphs, with a 15 dB amplitude for the bimorph attached directly to the shaker and a 5 dB amplitude for the other. The response flattens after this, until the final peak is reached at approximately 500 Hz. Here, the peak amplitude for both bimorphs is approximately 10 dB. Of additional note is a small 2 dB peak in the bimorph clamped to the rigid aluminum framework at approximately 350 Hz.

Analysis of this data, in particular the differentiation between peaks caused by the response of the test structure and those of the actual energy harvester, is ongoing.
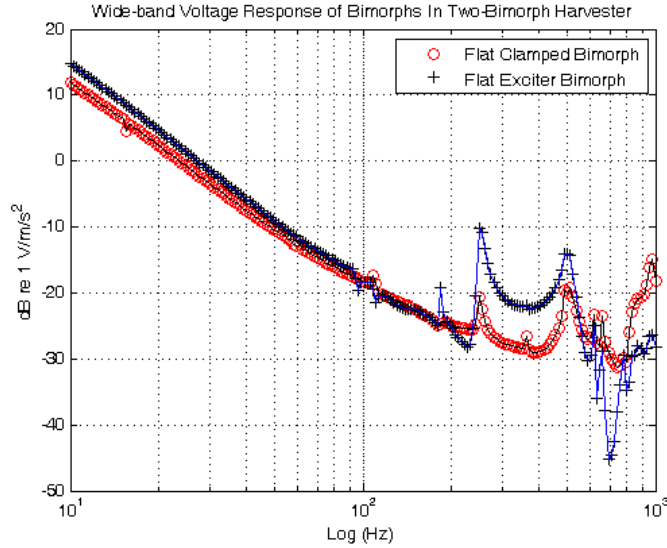

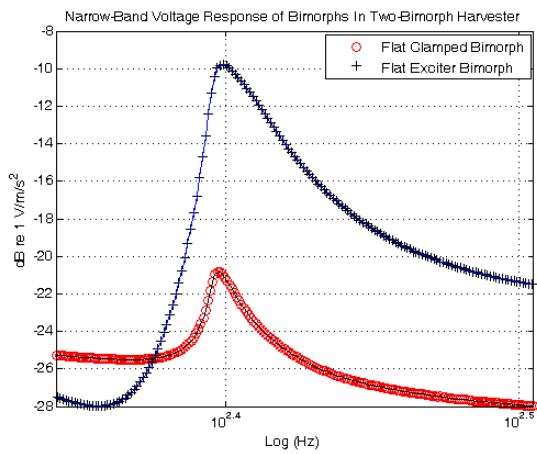Figure 12. Response of both bimorphs in two bimorph device to base excitation from 10 Hz – 1000 Hz

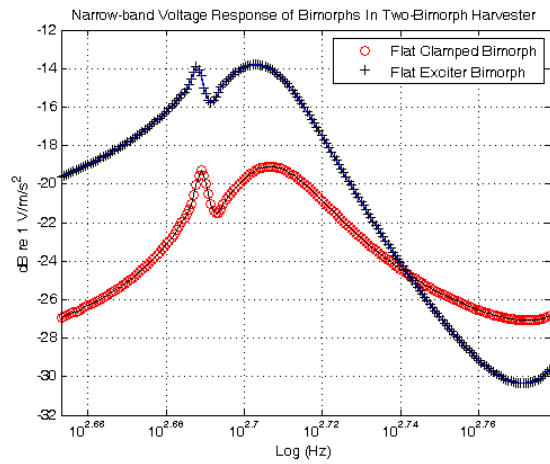Figure 13. Response of both bimorphs to base excitation from 220 Hz – 350 Hz

Figure 14. Response of both bimorphs to base excitation from 450 Hz – 600 Hz

4. CONCLUSION

Piezoelectric bimorph energy harvesters are widely studied and thoroughly understood [2,8]. Cantilever bimorph energy harvesters are the most common devices found in the literature, but suffer extensively from the "Gain-Bandwidth Dilemma" [7]. Generator arrays and clamped-clamped beams are alternative structures that have been shown to widen the bandwidth of energy harvesters [5, 7, 12, 15]. The energy harvester presented in this paper is a novel two-bimorph device with a connecting hinge. The hinge consists of a dowel pin and torsion spring that produces an additional moment on the bimorphs in response to rotation. To derive theoretical expressions for the two-bimorph device, a single bimorph cantilever is first modeled and tested. Good agreement is achieved for the single cantilever bimorph between model and experiment, although power dissipated in the measurement load is paltry without optimization. The two-bimorph device is modeled as an extension of the single bimorph device using Euler-Bernoulli Beam Theory and Circuit Laws. Modeling of the device is ongoing. The two-bimorph device is subject to a frequency sweep and the voltage response is obtained for known base excitation. Analysis of the response is ongoing, with particular interest in differentiating between features caused by the test structure and those caused by the energy harvester.

REFERENCES

[1] Burrow, S.G., L.R. Clare, A. Carella, and D. Barton. "Vibration Energy Harvesters with Non-linear Compliance." *Proceedings of the SPIE* (2008). Print.

[2] Erturk, A., and D.J. Inman. "A Distributed Parameter Electromechanical Model for Cantilevered Piezoelectric EnergyHarvesters." *Journal of Vibration and Acoustics* 130.4 (2008). Print.

[3] Erturk, A., and D.J. Inman. "An Experimentally Validated Bimorph Cantilever Model for Piezoelectric Energy Harvesting from Base Excitations." *Smart Materials and Structures* 18.1 (2009). Print.

[4] Erturk, A., D.J. Inman, and J. Hoffmann. "A Piezomagnetoelastic Structure for Broadband Vibration Energy Harvesting." *Applied Physics Letters* 94.25 (2009). Print.

[5] Ferrari, Marco, and Vittorio Ferrari. "Piezoelectric Multifrequency Energy Converter for Power Harvesting in Autonomous Microsystems." *Sensors and Actuators A: Physical* 142.1 (2008). Print.

[6] Gieras, J.F. Electromechanical Energy Harvesting System. Chubb International Holdings Limited (Sunbury-on-Thames, GB), assignee. Patent 20090079200. 26 Mar. 2009. Print.

[7] Hajati, Arman, and Sang-Gook Kim. "Ultra-wide Bandwidth Piezoelectric Energy Harvesting." *Applied Physics Letters* 99.8 (2011). Print.

[8] Kim, Miso, Mathias Hoegen, John Dugundji, and Brian L. Wardle. "Modeling and Experimental Verification of Proof Mass Effects on Vibration Energy Harvester Performance." *Smart Materials and Structures*19.6 (2010). Print.

[9] Lee, Ki Bang, Liwei Lin, and Young-Ho Cho. "A Closed-form Approach for Frequency Tunable Comb Resonators with Curved Finger Contour." *Sensors and Actuators A: Physical* 141.2 (2008): 523-29. Print.

[10] Nguyen, Son D., and Einar Halverson. "Nonlinear Springs for Bandwidth-Tolerant Vibration Energy Harvesting." *JMEMS Letters* 20.6 (2011). Print.

[11] "Piezoceramic Materials & Properties." *Piezo Systems: Piezoceramic, PZT, Piezoelectric Transducers, Piezoelectric Actuators and Sensors, Piezoelectric Fans, Piezoelectric Amplifiers, Piezoelectric Engineering, Ultrasonic Transducers, and Energy Harvesters*. Web. 08 Feb. 2012. <http://www.piezo.com/prodmaterialprop.html>.

[12] Shahruz, S.M. "Design of Mechanical Band-pass Filters for Energy Scavenging." *Journal of Sound and Vibration* 292.3-5 (2005): 987-98. Print.

[13] Weinberg, Marc S. "Working Equations for Piezoelectric Actuators and Sensors." *Journal of Microelectromechanical Systems* 8.4 (1999). Print.

[14] Wu, Xiaoming, Jianhui Liu, Seiki Kaoto, Kai Zang, Tianling Ren, and Litian Liu. "A Frequency Adjustable Vibration Energy Harvester." *Proceedings of PowerMEMS* (2008). Print.

[15] Xue, Huan, Yuantai Hu, and Qing-Ming Wang. "Broadband Piezoelectric Energy Harvesting Devices Using Multiple Bimorphs with Different Operating Frequencies." *IEEE Transactions on Ultrasonics, Ferroelectrics and Frequency Control* 55.9 (2008): 2104-108. Print.

[16] Zhu, Dibin, Michael J. Tudor, and Stephen P. Beeby. "Strategies for Increasing the Operating Frequency Range of Vibration Energy Harvesters: A Review." *Measurement Science and Technology* 21.2 (2010): 022001. Print.